Research Square

Preprints are preliminary reports that have not undergone peer review.
They should not be considered conclusive, used to inform clinical practice,
or referenced by the media as validated information.

Additively Manufactured Rectilinear Infilled Carbon-Fibre-Reinforced Polyamide Composite Architectures for Next-Generation Lightweight Wind Turbine Blades

Akash Jain
Indian Institute of Technology Mandi
Satinder K. Sharma
satinder@iitmandi.ac.in

Indian Institute of Technology Mandi

Research Article

Keywords: wind turbine blades, material extrusion, lightweight, rectilinear infill, renewable energy materials

Posted Date: August 24th, 2026

DOI: https://doi.org/10.21203/rs.3.rs-10633593/v1

License: This work is licensed under a Creative Commons Attribution 4.0 International License.
Read Full License

Additional Declarations: No competing interests reported.

Additively Manufactured Rectilinear Infilled Carbon-Fibre-Reinforced Polyamide Composite Architectures for Next-Generation Lightweight Wind Turbine Blades

Abstract

The growing mandate for sustainable energy systems has increased the need for lightweight, durable, and high-performance materials for next-generation wind turbine blade applications. Although additive manufacturing (AM) has emerged as a promising route for fabricating complex composite structures, the thermal and mechanical behaviour of rectilinear-infilled carbon fibre-reinforced polyamide (CFPA) composites fabricated via fused filament fabrication (FFF) AM for architectural compatibility and lightweight wind turbine blade applications remain largely unexplored. In this study, FFF-printed rectilinear infilled CFPA composites were investigated due to efficient load transfer and structural stiffness for lightweight wind turbine blade. CFPA (commercially known as Onyx), combines the toughness of polyamide (PA) with the enhanced mechanical strength of chopped carbon fibre (CF) reinforcement; specimens were fabricated using process flows, including ±45° raster orientation, 0.10 mm layer thickness, 100% rectilinear infill density, and controlled thermal settings. Thermogravimetric analysis revealed excellent thermal stability and delayed degradation behaviour due to effective CF reinforcement within the PA matrix. X-ray diffractometry analysis confirmed the presence of a stable semi-crystalline structure with improved intermolecular bonding and structural integrity. Mechanical characterisation depicts an average tensile strength of ~33.5 MPa, compressive strength of ~72.2 MPa, impact strength of ~42.1 kJ/m², and flexural strength up to ~33 MPa, indicating reliable load-bearing capability and energy absorption characteristics. Hardness and surface morphology studies further confirmed the dimensional consistency and surface stability of the printed composites, with an average surface roughness value of ~ 8.65 µm. The results indicate that FFF-based rectilinear CFPA composites exhibit promising thermal durability, mechanical strength, and energy absorption for lightweight wind turbine blade structures with reduced material wastage and enhanced AM flexibility.

Keywords: wind turbine blades; material extrusion; lightweight; rectilinear infill; renewable energy materials.

1. Introduction

Wind energy is the most favoured type of energy because of its clean nature and its ability to help reduce contamination due to fossil fuels [1–3]. Wind energy serves as a feasible substitute for fossil fuels, exhibiting superior efficiency compared to other renewable energy sources, including biomass and tidal energy, and incurs lower prices than photovoltaic electricity [4,5]. In response to the escalating unfavourable effects of fossil fuels, numerous countries have begun developing renewable alternatives such as solar and wind power etc. [6]. The wind turbine blades are the principal structural components of the wind turbine system and endure diverse structural loads during their operational lifespan. In recent years, additive manufacturing (AM) has developed as a viable method for the creation and optimisation of mechanically robust and ecologically durable wind turbine blades, as seen in FIGURE 1. AM provides substantial benefits, including design versatility, minimised material waste, expedited prototyping, lightweight structural production, and the capability to create intricate shapes that are challenging to manufacture using traditional methods [7].

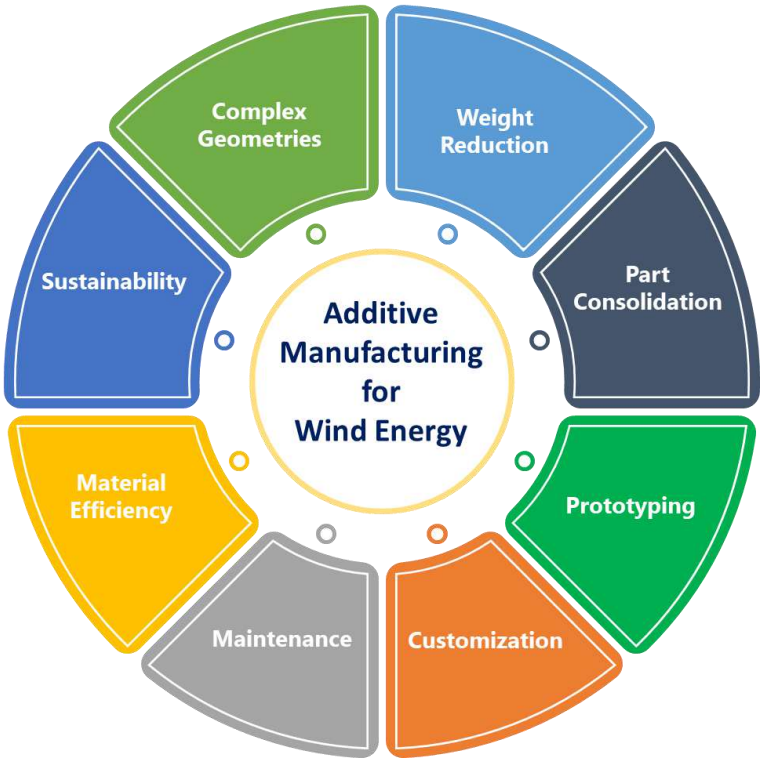


FIGURE 1 Scope of AM in wind energy.

The AM approach, namely material extrusion-based fused filament fabrication (FFF), has garnered interest due to its cost-efficacy, satisfactory dimensional accuracy, ease of processing, and capacity to create geometrically intricate structures [6,8]. The FFF processing factors influence the quality of manufactured goods, including part orientation on the printing

platform, infill density, infill pattern, wall count, layer thickness, and the incorporation of reinforcing fibres [9,10]. Therefore, it is essential to characterise mechanical behaviour by evaluating the impact of specific processing parameters, particularly component orientation and placement on the printing platform, which also affect their mechanical behaviour, as well as geometric quality [11,12]. The FFF factors utilised in the fabrication process must be examined to enhance mechanical and energy-absorption properties, optimise interlayer adhesion in the printed composite, minimise dimensional tolerances, and decrease porosity of the layers [13,14]. Polymeric composite materials are extensively utilised in high-performance components [15–17]. The choice of polymer base and reinforcement materials significantly influences the mechanical behaviour of the fabricated components [18–20]. Fibre-reinforced polymeric composites have improved strength and enhanced durability compared to particle-reinforced polymer composites [21]. Frequently utilised polymer base matrix materials for fiber-reinforced polymer composites include polylactic acid (PLA), acrylonitrile butadiene styrene (ABS), and polyamide (PA), among others [22–24]. The PA matrix offers higher mechanical qualities, excellent durability, improved affinity with fibres reinforcement, and exceptional chemical endurance [25]. Buj-Corral et al. indicated that FFF- printed PA spur gears exhibited a reduced level of form error compared to PLA [26]. Yankin et al. [27] investigated the fatigue behaviour of FFF- printed PA and ABS components, finding that the PA parts exhibit a steeper slope compared to the ABS parts. The tri-hexagon structure contributes to an increased fatigue life [27]. Guessasma et al. [28] reported that FFF-printed polyamide (PA) parts can be effectively fabricated at nozzle temperatures between 250°C and 255°C, resulting in improved mechanical and thermal properties. Moreover, surpassing the temperature range diminishes the rigidity and tensile strength of the polymer components [28]. Carbon fibre (CF) is the predominant fibre reinforcement, alongside glass, Kevlar, rayon, and polyester, due to its enhanced dimensional stability, superior stiffness-to-strength ratio, weight reduction, enhanced dimensional stability, and increased thermal and electrical properties [29]. The CF-reinforced PA (CFPA) (commercially known as Onyx) is an advanced thermoplastic composite that has gained widespread adoption due to its higher strength, superior toughness, enhanced wear resistance, improved surface finish, and better dimensional accuracy compared with unreinforced polymer systems [30,31]. This engineered composite has excellent thermal stability and can be heated, reshaped, and cooled repeatedly without significant degradation of surface finish and structural integrity in FFF-printed parts, ensuring long-term durability and reusability. Piramanayagam et al. [32] assessed the influence of infill patterns and densities on the tensile properties of FFF-printed CFPA specimens and reported that higher infill density,

while rectilinear, is noted to exhibit superior tensile strength and energy absorption. Nikiema et al. [33] examined the influence of process parameters and humidity on the mechanical properties of FFF-manufactured CFPA composites, reporting that the mechanical characteristics varied by approximately 10% across different printing orientations.

Peng et al. [34] investigated short and continuous CFPA composites for energy absorption characteristics and reported that a continuous fibre raster angle of ± 45° exhibits a maximum energy absorption. The CF-reinforced composite lattice structure is widely used in aeronautical, civil, and mechanical engineering due to its high strength-to-weight ratio, excellent impact resistance, corrosion protection, and superior mechanical and energy absorption properties compared to conventional polymeric lattice structures [35–37].

Das et al. [38] examined the effect of FFF process factors, including layer height, nozzle temperature, and deposition rate, on the tensile behaviour of unmodified PA and CFPA materials. Extruded CFPA beads demonstrate superior form retention compared to pristine PA material across the examined temperature range, attributed to their elevated zero-shear viscosity. Anbalagan et al. [39] conducted an independent study examining the impacts of construction characteristics, including infill density and patterns, on both FFF-printed tensile and flexural CFPA specimens and reported that topologically optimised models of certain patterns exhibit superior performance compared to unoptimized models with increased infill densities, due to enhanced bonding of the patterns. Sangaletti et al. [40] explored the impact of various arrangements of printing orientations and raster angles on the surface roughness of fractures, mechanical performance, fracture toughness, and fracture processes at the mesoscale of FFF-printed CFPA specimens. Voids are common defects in parts fabricated through FFF, mainly because adjacent filaments and layers may not completely fill with each other [31]. These internal gaps can reduce the effective load-bearing area and generate local stress concentrations, which may negatively affect the strength, stiffness, and overall mechanical performance of printed components [41]. In fibre-reinforced composites, additional voids may occur within the deposited bead due to incomplete material flow and fibre–matrix interactions [42]. Therefore, evaluating the void fraction is important for understanding the internal quality of printed composites. SEM-based image analysis offers an effective approach to observe void morphology and estimate the porosity level in the printed structure [43].

In the view of literature on FFF-printed polymer composites and CFPA materials, it is evident that optimising printing process parameters and lattice structures is crucial for enhancing the functional behaviour, dimensional stability, and structural integrity of composite components, comprehensive investigations focused on rectilinear infilled CFPA structures for wind turbine

blade applications remain limited, particularly, correlated thermo-mechanical behaviour, structural integrity, surface characteristics, renewable-energy-oriented performance of FFF-printed CFPA composites and the applicability of rectilinear infill architectures for enhancing load distribution, dimensional stability, and energy absorption in lightweight wind turbine blade structures has not been appropriately explored. Therefore, this work focuses on the development and characterisation of rectilinear lattice-integrated CFPA structures by analysing thermogravimetric behaviour, X-ray diffractometry, tensile, compression, impact, and flexural behaviour, hardness, and surface roughness to achieve high-performance wind turbine blade structures. Also aims to establish the suitability of rectilinear CFPA architectures for renewable-energy applications that require lightweight characteristics, structural reliability, enhanced energy absorption, and manufacturing flexibility.

2. Materials and Method

This section addresses the various materials and methods employed in composite development and their characterisation.

2.1. Materials

This study seeks to ascertain the functional behaviour of components manufactured using CFPA materials (black filament of diameter 1.75±0.02 mm), produced in roll form and provided by Markforged. The CFPA, commercially referred to as Onyx, is a polymer alloy containing roughly 10% to 20% by volume of tiny carbon fibres. The length of CF in CFPA ranges from 7.035 to 44.58 μm, with fibres predominantly aligned along the material's deposition direction [44]. The CFPA material facilitates superior precision and outstanding surface quality in the manufactured components. It possesses beneficial mechanical characteristics and chemical resistance. Before printing, the filament was stored under controlled conditions to minimise moisture absorption, and moisture conditioning was maintained at a controlled relative humidity. The filament was dried before fabrication to ensure consistent extrusion and reduce moisture-related defects. The printer was properly calibrated before each fabrication batch, including verification of bed alignment, extrusion and temperature settings. The build orientation was kept constant for all specimens to ensure consistent material deposition and mechanical behaviour. CFPA provides good dimensional accuracy, surface quality, mechanical performance, and chemical resistance, making it suitable for functional components manufactured through additive manufacturing.

2.2. Fabrication of testing specimens

The test specimens were produced utilising the Markforged Mark Two (Gen 2) industrial-grade FFF printer, capable of manufacturing components within a volume of 132 mm × 320 mm ×

154 mm, ensuring adherence to industrial-quality requirements. The computer-aided design (CAD), FIGURE 2, was developed utilising SOLIDWORKS, and the printing parameters were established utilising Simplify3D software. The shape is sliced to generate the G-code for the Markforged Mark Two (Gen 2) FFF configuration. The specimens were fabricated in sets of three using a 0.4 mm nozzle to maintain consistent and repeatable printing conditions. A ±45° raster orientation was selected to provide balanced load distribution in the printed structure. The 260°C nozzle temperature and 90°C bed temperature were maintained to ensure proper material flow and adhesion. A 0.10 mm layer thickness was used to achieve good printing resolution and interlayer bonding. Three perimeters and 100% rectilinear infill were applied to obtain dense specimens with minimal internal gaps. The specimens were printed at a 20 mm/s fabrication speed with XY-plane placement to ensure consistent fabrication conditions.

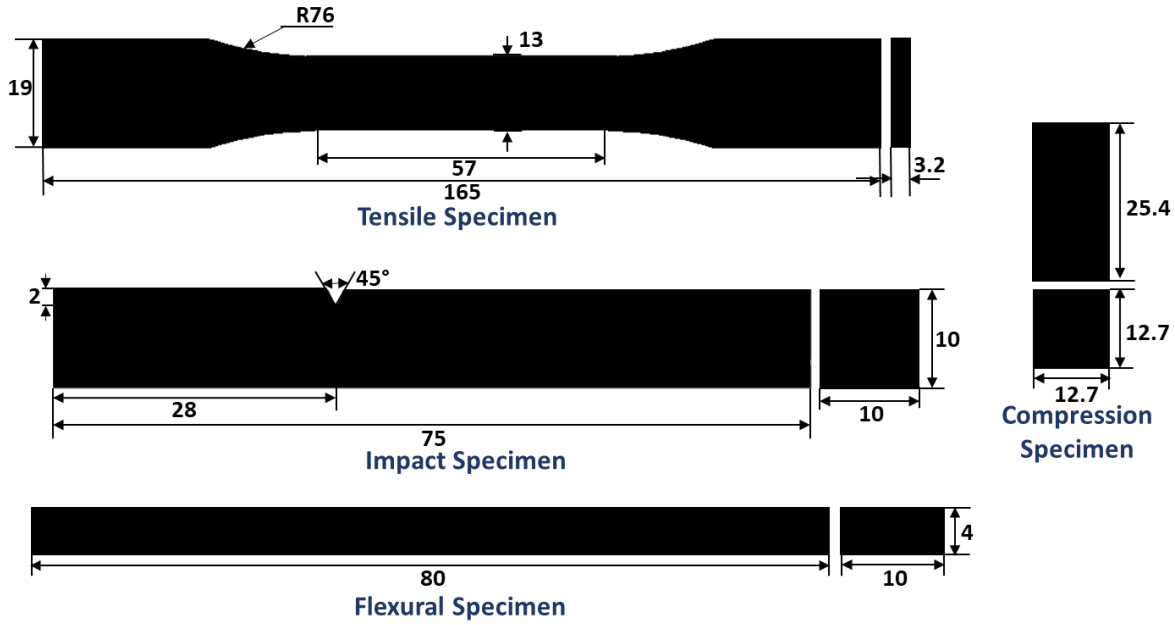


FIGURE 2 Dimensions of Different Testing Specimens.

2.3. Thermogravimetric Analysis

The specimen was evaluated using a NETZSCH STA 449 F1 Jupiter thermogravimetric analyser. The temperature of the samples was elevated from 25 to 500°C at a rate of 5°C/min in a nitrogen environment. The gathered data was utilised to ascertain the volume percentages of the CFPA filaments.

2.4. X-Ray Diffractometry

X-ray diffractometry (XRD) is a procedure that use the scattering of X-rays by crystalline substances to ascertain their structural attributes, such as phase composition, grain size, and orientation, through the analysis of diffraction patterns. This entails quantifying the intensities of diffracted rays, which correlate with the atomic arrangement within the crystal. The XRD

study was conducted utilising a Rigaku MiniFlex X-ray diffractometer. The patterns were obtained within a scanning range of 0°–100° in 2θ, with a step size of 0.01° and a scanning rate of 1.00°/min.

2.5. Tensile Behaviour

The tensile strength was evaluated under standard conditions utilising a Tinius Olsen H50KS Material Testing Machine capable of with a 50 kN load. Tensile testing was conducted at a constant crosshead velocity of 2 mm/min, with three specimens, and the results were averaged for accuracy. The production of dumbbell-shaped specimens with ASTM D638 standard, guaranteeing reliability in the testing procedure.

2.6. Compressive Behaviour

Compression tests were performed in compliance with ASTM D695 standards. Compression testing is performed via a Tinius Olsen H50KS Material Testing Machine, which has a maximum capacity of 50 kN. Compression testing was conducted at a constant crosshead velocity of 2 mm/min. This entails exerting compressive stress on the specimen via specialist fixtures in advanced universal testing equipment. The procedure includes placing the test specimen between two plates for compression testing. During the examination, the specimen is subjected to compression, revealing the relationship between stress and strain. This data is essential for evaluating the compressive strength of the analysed specimen.

2.7. Impact Behaviour

An Izod impact testing apparatus was utilised to evaluate the impact behaviour of the specimens in line with ASTM D256 standards, employing an Advance Equipment ICIT impact test instrument. In this experiment, a pendulum with a predetermined potential energy is raised to a specified height and then released to fall. The specimen is impacted upon collision with the notched area while positioned in the pendulum's path. The notch is intrinsic to the created specimens, having been integrated into the original specimen design.

2.8. Flexural Behaviour

The three-point flexural test was performed using ASTM D790 standards to determine flexural strength. Specimens were evaluated with the Tinius Olsen H50KS Material Testing Machine, possessing a capacity of 50 kN, with a loading beam positioned centrally between two supporting beams separated by 64 mm. Flexural testing was conducted at a constant crosshead velocity of 2 mm/min.

2.9. Hardness Behaviour

The hardness of printed specimens was assessed using the Hysitron TI 950 nanoindentation technology. Prior to the commencement of the test, the specimens were positioned on a stable,

immovable surface. The indenter needle was applied vertically to the test specimen, and the recorded reading was noted once the pressure foot made complete contact with the specimen surface. The dimensions of the test specimen were preserved at 10 mm × 10 mm × 10 mm.

2.10. Surface Roughness

The surface roughness (Ra) of the specimens was assessed using a Bruker Contour GT-K in accord with the ISO 4288:1996 standard [45]. This parameter was assessed five times for each specimen in the 0° direction and five times in the 90° direction.

2.11. Void Fraction

Void fraction was determined from SEM images obtained from the cross-sections of the FFF specimens by utilizing the MATLAB Image Processing Toolbox to perform image processing, visualization, and analysis. The images were initially converted into grayscale and enhanced to obtain clear contrast between the material and darker void regions. Then an intensity-based threshold was used to isolate the voids from the surrounding matrix. The void fraction was expressed as the percentage of void area relative to the total analysed cross-sectional area [43].

3. Results and Discussion

3.1. Thermogravimetric Analysis

The thermogravimetric (TGA) plot of the FFF-printed CFPA composite demonstrates highly favourable thermal stability characteristics, confirming its strong potential for wind turbine blade applications. This behaviour reflects the thermal robustness of the CFPA and highlights the effectiveness of the FFF process in producing a structurally stable composite material. For wind turbine blades, thermal stability is a critical parameter because the blades are continuously exposed to varying environmental temperatures, solar radiation, frictional heating, and long-term outdoor operating conditions [46]. The TGA response indicates that incorporating chopped CFs into the polyamide matrix effectively delays thermal degradation and improves the thermal endurance of the composite system. The initial section of the TGA curve, where minimal weight loss occurs, signifies that the material possesses low moisture absorption and strong resistance to early-stage thermal decomposition. This is particularly advantageous for wind turbine systems operating in humid, coastal, and fluctuating climatic environments [47]. The stable mass profile at lower and intermediate temperatures confirms that the FFF-printed CFPA can retain its structural integrity during normal service conditions without experiencing premature material degradation. Such thermal resistance contributes directly to the reliability and durability of turbine blades during long-term continuous operation under outdoor service conditions [48].

The major decomposition region observed at elevated temperatures indicates the high degradation threshold of the composite material. This delayed thermal decomposition behaviour reflects strong intermolecular bonding within the PA matrix and effective reinforcement provided by the embedded CFs. The presence of CF reinforcement improves thermal resistance by slowing degradation and enhancing heat dissipation [49]. For wind turbine blades, this improved thermal endurance is beneficial because it helps maintain mechanical performance and dimensional stability under cyclic thermal loading and prolonged environmental exposure. In wind turbine blade applications, the CF residue reflects the material's capability to sustain structural reinforcement even under severe thermal conditions, thereby improving safety, reliability, and long-term operational performance.

3.2. X-Ray Diffraction Analysis

The X-ray diffraction (XRD) behaviour of the FFF-printed rectilinear CFPA composites confirms the presence of a stable semi-crystalline structure with improved molecular ordering and reinforcement interaction.

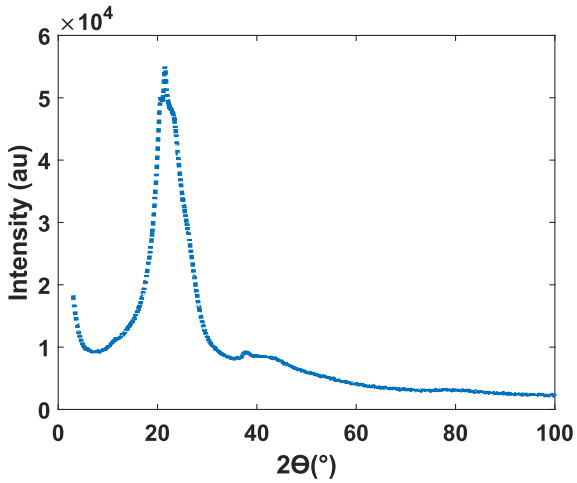


FIGURE 3 XRD Characterisation of FFF-printed CFPA.

FIGURE 3 demonstrates a prominent and intense peak in the lower 2θ region (21.54°), which indicates the presence of a well-organised semi-crystalline structure in the CFPA. This strong diffraction behaviour validates the successful preservation of the internal molecular arrangement of the material by the FFF process resulting in enhanced structural stability and reliable material performance. This structural consistency is very important for wind turbine blades because the blades are constantly exposed to fluctuating aerodynamic loads, rotational stresses and varying environmental conditions.

The dominant peak in the XRD plot indicated an increased crystallinity of the CFPA material. Higher crystallinity translates to better mechanical properties, such as enhanced stiffness, dimensional stability, and load-bearing capability [50]. This is especially beneficial for wind

turbine blades, where the ability to maintain an aerodynamic shape and resist deformation is key for efficient energy generation. The sharpness and intensity of the peak also indicate strong intermolecular bonding and effective layer consolidation during the FFF process. This suggests that the printed layers were well fused and had fewer internal defects, thereby enhancing the overall structural integrity of the fabricated component. Apart from the crystalline behaviour, the broad background region in the diffraction pattern shows the presence of controlled amorphous phases in the composite. This balanced semi-crystalline structure is very useful because it offers a combination of stiffness and toughness. The crystalline regions provide strength and load-bearing ability, while the amorphous regions allow it to absorb impact energy and reduce brittleness [51]. Such a combination is important for wind turbine blades that must endure cyclic loading and dynamic wind forces over long periods of time. The fatigue life and in-service reliability can be significantly improved by the ability of the material to resist crack initiation and propagation [52]. The uniform and smooth nature of the diffraction pattern also indicates that there is no major thermal degradation during printing. This indicates that the selected FFF parameters were well optimised and produced a stable composite structure with uniform material distribution. The improved diffraction response indicates the effective incorporation of chopped CF reinforcement within the PA matrix, thus confirming the improved reinforcement interaction and overall composite performance.

3.3. Tensile Analysis

The tensile behaviour of FFF-printed rectilinear CFPA composites demonstrates relatively consistent stress–strain characteristics under optimized processing conditions.

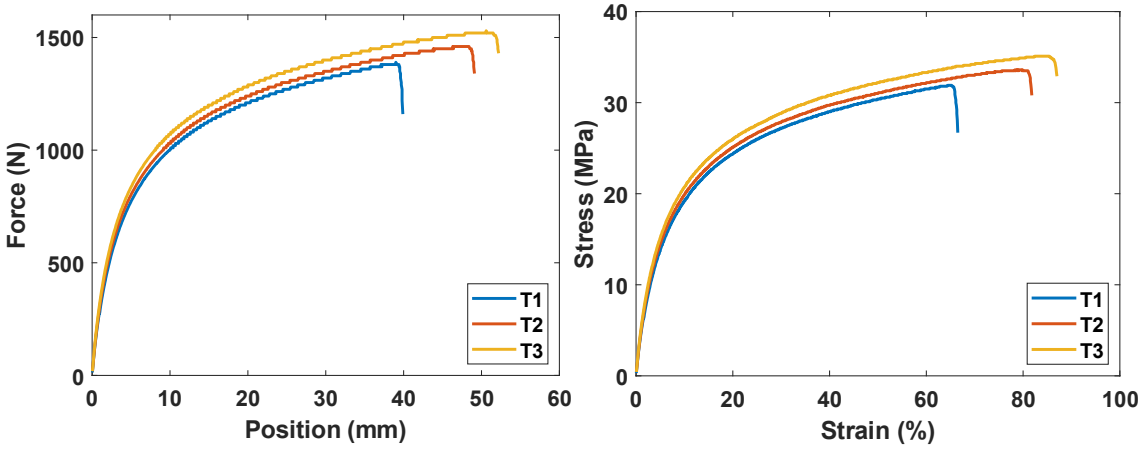


FIGURE 4 Tensile Behaviour of FFF- printed CFPA material.

The stress-strain profiles for the tensile specimen are depicted in FIGURE 4. All three specimens demonstrate comparable elastic behaviour and nearly identical yield and ultimate stress, with an average tensile strength of 33.5 MPa. The alignment of yield and final stress

signifies a lack of substantial plastic deformation, consistent with a predominantly brittle failure mechanism. This observation is additionally supported by the pronounced stress drop, while minor step-like fluctuations indicate localised progressive degradation mechanisms, such as interlayer debonding.

The inequality in ultimate force and total elongation indicates slight inconsistencies in filament deposition and interlayer adhesion. The ±45° raster orientation facilitates a more equitable load distribution under tensile forces, advantageous for applications subjected to multidirectional pressures. The comparatively elevated elongation values, in contrast to standard brittle polymer chains mobility, and the stress concentration effects induced by CF reinforcement and interlayer interfaces, further indicate that the chopped CF-reinforced PA matrix possesses a degree of ductility, facilitating energy absorption before breakdown [53].

In the context of wind turbine blade applications, these findings demonstrate that FFF-printed CFPA can deliver reliable tensile strength and stiffness when manufactured under optimised conditions, making it suitable for lightweight structural components. The selected raster architecture likely enhanced filament interlocking and reduced directional anisotropy compared with unidirectional deposition strategies. The observed diversity in elongation and the brittle characteristics of final failure underscore possible limitations under cyclic and torsional loading conditions characteristic of turbine operation. Consequently, although the material demonstrates potential for small-scale and prototype blades, attention to structural design, load orientation, and potential reinforcement techniques is essential to ensure long-term durability and reliability.

3.4. Compression Behaviour

The compression behaviour of the FFF-printed rectilinear CFPA composites demonstrates stable load-bearing capacity and progressive deformation under compressive loading.

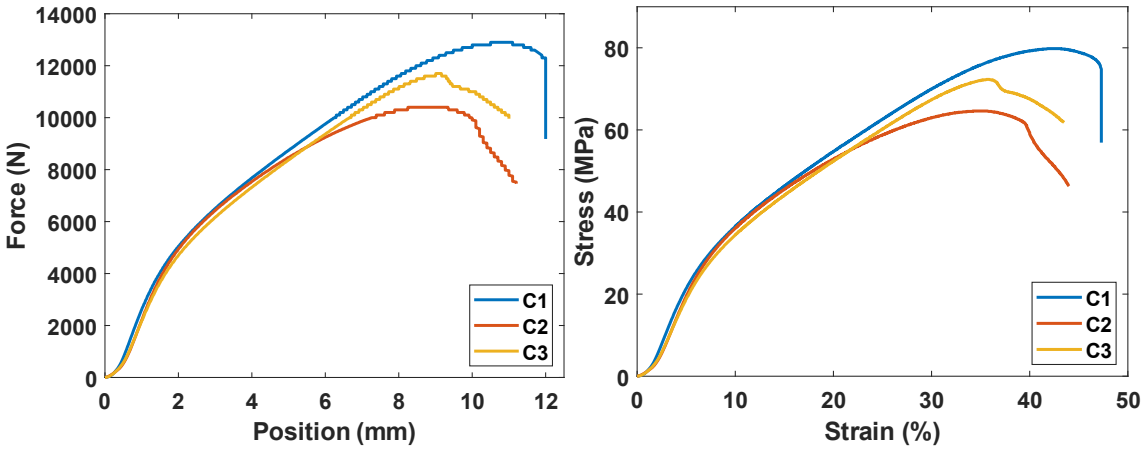


FIGURE 5 Compression Behaviour of FFF- printed CFPA material.

The compression behaviour of FFF-printed CFPA demonstrates a relatively stable yet moderately scattered response under identical processing parameters, highlighting the reliability of the structures. The stress–strain curves in FIGURE 5 show that the specimens follow a trend, beginning with a linear elastic region and transitioning into a nonlinear deformation phase before reaching peak stress. The compressive strength varies from 64.6 MPa to 79.8 MPa, with an average of 72.2 MPa. It is observed in the ultimate force values, ranging from 10421.7 N to 12875.0 N, suggesting that load-bearing capacity under compression is influenced by localized structural inconsistencies.

The failure under compression is more progressive compared to tension, with smoother transitions rather than abrupt drops, indicating mechanisms such as micro-buckling, layer-wise crushing, and gradual densification of the material. The material does not exhibit a well-defined yielding phase but instead transitions directly into failure, which is characteristic of stiff, fibre-reinforced thermoplastic systems. For wind turbine blade applications, these results are particularly relevant, as compressive loads are critical on the blade during operation. The relatively high compressive strength of CFPA is advantageous for maintaining structural integrity. Therefore, while the material shows promising compressive performance and energy absorption characteristics, ensuring uniform print quality and optimizing process parameters are essential to achieve reliable and consistent behaviour in real-world turbine blade applications [54].

3.5. Impact Behaviour

The impact behaviour of FFF-printed CFPA demonstrates a reasonably consistent energy absorption capacity under identical processing parameters. The absorbed energy values range from 0.65 to 0.73 kg-m, with an average of 0.69 kg-m, while the impact strength varies between 39.7 and 44.2 kJ/m², averaging 42.1 kJ/m². This relatively narrow spread indicates that the material exhibits stable impact performance when produced under controlled conditions.

The specimens' impact behaviour indicates that small differences in internal structure, including interlayer bonding quality, filament fusion, and the presence of micro voids, can influence the material's ability to absorb and dissipate impact energy [41]. It can be associated with progressive energy-dissipation mechanisms rather than shattering failure, implying that the material possesses a degree of toughness despite its layered structure.

The consistent impact strength suggests that FFF-printed CFPA can provide reliable resistance to such phenomena. The material demonstrates adequate and repeatable impact performance,

making it a viable candidate for such applications, if process parameters are carefully optimised to enhance toughness and reduce structural inconsistencies.

3.6. Flexural Behaviour

The flexural behaviour of the FFF-printed rectilinear CFPA composites demonstrates stable bending resistance and progressive deformation characteristics under three-point loading conditions.

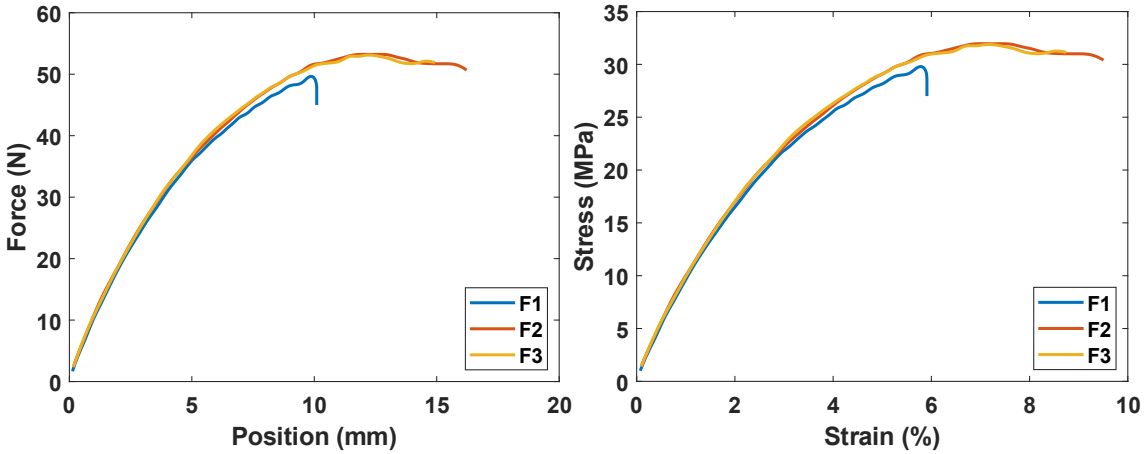


FIGURE 6 Flexural Behaviour of FFF- printed CFPA material.

FIGURE 6 exhibits the three-point flexural behaviour of FFF-printed CFPA. The load-deflection trends for all three specimens follow a similar trajectory, beginning with a linear elastic region and gradually transitioning into a nonlinear phase before reaching peak load. This indicates stable flexural stiffness, suggesting that the printing parameters provide reasonably uniform resistance to bending.

The ultimate flexural strength increases from 30.0 MPa to 33.0 MPa, and the corresponding ultimate force rises from 50.0 N to 55.0 N, indicating a limited but noticeable variation in load-bearing capacity within the same parameter set. Similarly, total elongation ranges from 5.9% to 9.5%, reflecting good ductility and deformation capability. FIGURE 6 depicts a gradual failure mechanism, with smooth drops in load, indicating progressive damage, such as tensile cracking on the outer surface and interlayer delamination, rather than a sudden fracture.

For wind turbine blade applications, where bending loads are dominant due to aerodynamic forces, these results indicate that FFF-printed CFPA can provide stable flexural stiffness and adequate strength. The material is suitable for bending-dominated applications, ensuring consistent print quality and optimizing internal structure are crucial to enhance reliability and long-term performance under cyclic loading conditions [55].

3.7. Hardness Characterisation

The hardness behaviour of FFF-printed CFPA demonstrates a relatively consistent response under identical processing parameters, indicating good repeatability of FFF-printed specimens. The measured hardness values range from 78.6 to 84.1, resulting in an average hardness of 81.7. This narrow spread suggests that the material exhibits stable surface resistance to localized deformation when processed under controlled conditions.

From an application perspective, particularly for wind turbine blades, hardness plays an important role in determining resistance to surface wear, erosion, and minor impact damage caused by airborne particles. The relatively uniform hardness values observed here suggest that FFF-printed CFPA can provide dependable surface durability across the component. The results indicate that FFF-printed CFPA possesses adequate and reproducible hardness characteristics suitable for such applications, while emphasizing that minimizing internal defects and ensuring uniform layer bonding are essential for enhancing long-term surface reliability under operational conditions.

3.8. Surface Roughness Analysis

The surface morphology analysis of the FFF-printed rectilinear CFPA composites demonstrates relatively uniform material deposition and consistent layer formation during fabrication.

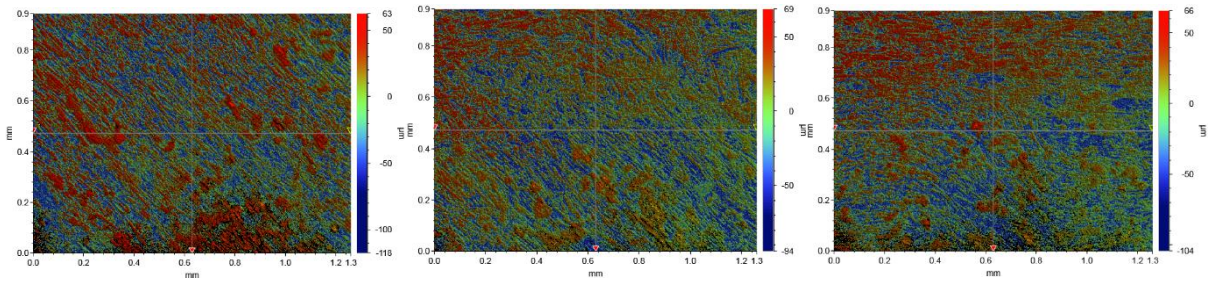


FIGURE 7 Surface Roughness of FFF- printed CFPA material.

FIGURE 7 show the promising surface properties of the FFF-printed CFPA material. The average surface roughness (Ra) value of 8.65 µm indicates a moderately textured but highly functional surface, especially for aerodynamic structures. The distribution of peaks and valleys in the 3D surface contour maps appears fairly uniform throughout the scanned region, suggesting good layer adhesion and consistent deposition throughout the printing process. Such homogeneity strongly indicates the manufacturing process stability and demonstrates CFPA composite printing's ability to produce reliable structural surfaces suitable for engineering applications. Periodic undulations are evident, but the fluctuations remain within a controllable range, suggesting that the printing process has avoided abrupt unevenness and major defects. This controlled roughness can benefit wind turbine blade performance by enabling better mechanical interlocking between layers, thereby enhancing structural integrity and resistance

to delamination under cyclic wind loading [56]. The profiles also show that the surface features are evenly distributed rather than concentrated in isolated areas, which is beneficial for predictable aerodynamic behaviour across the entire blade surface. The measured roughness indicates that the printed CFPA surface is sufficiently smooth to minimise excessive airflow disruption while maintaining the inherent benefits of textured composite surfaces. In real wind turbine operation, this balance can help maintain stable airflow characteristics and increase the overall efficiency of the blades [57]. Also, the absence of severe spiking on the surfaces in the plots indicates a lower likelihood of stress concentration points, which directly results in better long-term fatigue performance and durability [57].

3.9. Void Fraction Analysis

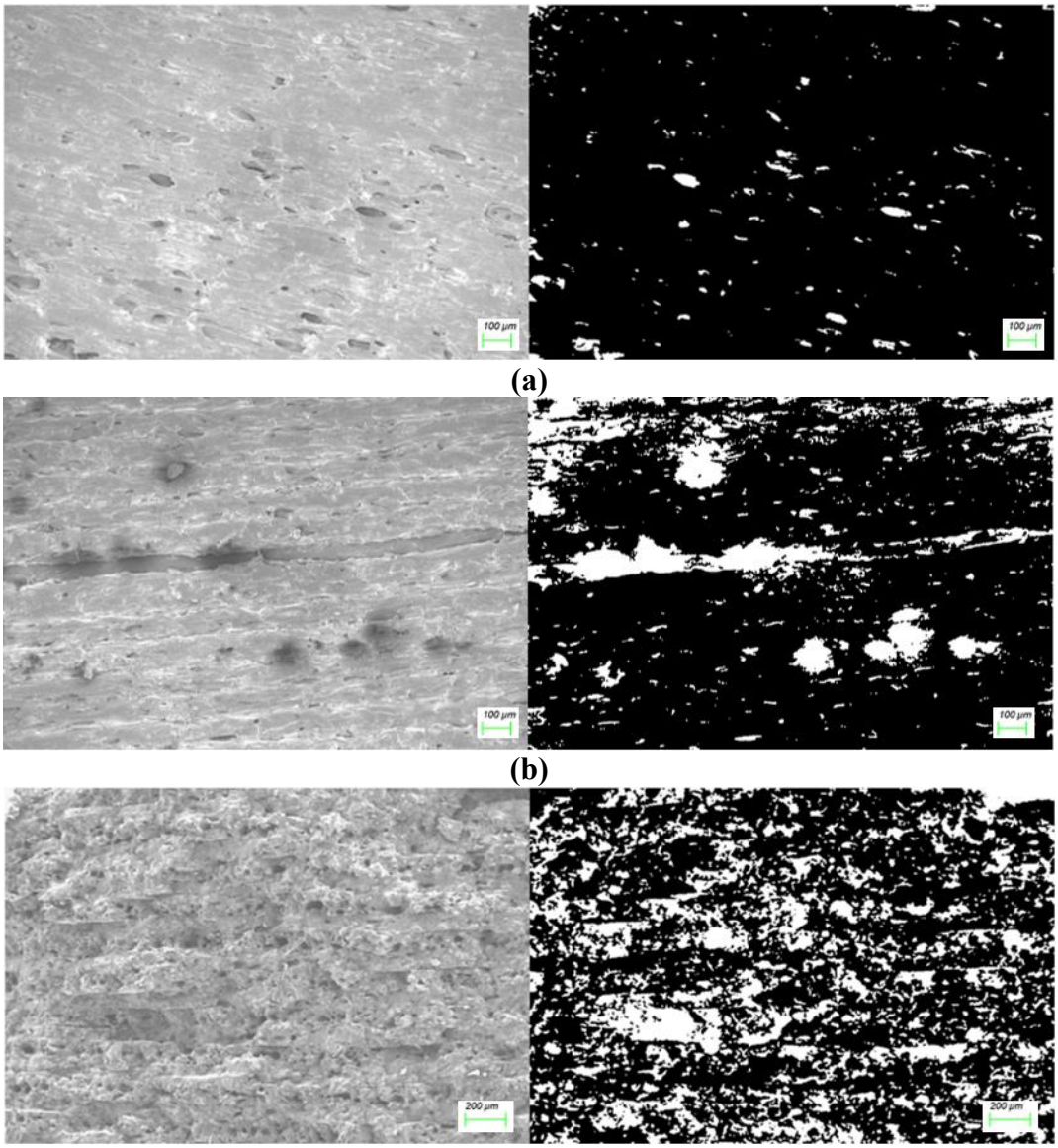


FIGURE 8 FESEM and Void Mask Image for Calculating the Void Fraction (a) Top Surface, (b) Layer wise, (c) Horizontal Fractured.

Three types of cross-sectional images, top surface image, layer-wise image and horizontal fractured image were studied, FIGURE 8. The measured average void fractions were ~10.75%, ~13.92% and ~17.36%, respectively. The top surface indicated a low void fraction of 10.75%, which means good material deposition and fusion in the layers. It indicates well-bonded deposited filaments and fewer surface defects, FIGURE 8(a). However, the layer-wise section revealed a void fraction of 13.92%, which indicates the presence of interlayer gaps due to improper bonding between consecutive deposited layers, FIGURE 8(b). Such defects are typical for FFF where each layer is deposited separately, and the bonding depends on thermal history and cooling rate [58]. The highest void fraction of ~17.36% was observed in the horizontal cut region, indicating that the internal voids are more intensive in the specimen than those on the external surface, FIGURE 8(c). These internal defects are mainly related to CF pullout and fusion between neighbouring raster lines, small variations in the extrusion and air trapped during the deposition of the CFPA. The increase in internal void content may lead to reduction of the effective load-bearing area and serve as sites for stress concentration which would decrease, the mechanical strength and fatigue resistance [42].

Internal voids are particularly important in the case of spiral wind turbine applications as the blades are exposed to continuous cyclic loading, with bending and changing aerodynamic forces during operation [58]. Excessive voids can cause crack formation and promote failure under repeated loading conditions and operations [59].

3.10. Structural Relevance for Wind Turbine Blade Applications

The experimental results collectively demonstrate that the FFF-printed rectilinear CFPA composites possess a balanced combination of lightweight characteristics, thermal stability, mechanical strength, impact resistance, and structural integrity suitable for renewable energy applications. Impact, tensile, compression, and flexural testing are critical in wind turbine blade applications to evaluate the structural integrity, durability and operational consistency of the blade components. Impact behaviour helps determine a material's resistance to sudden external forces, such as airborne debris, hail, dust particles, and unexpected loading conditions encountered during turbine operation. Knowledge of the blade material's impact resistance is important to ensure the blade can absorb and dissipate energy effectively without catastrophic failure.

Compression testing evaluates the capability of the material to resist compressive loads imposed by aerodynamic pressure and rotational forces acting on the spiral blade during continuous operation. Similarly, flexural testing is important because wind turbine blades are always subjected to bending loads from wind pressure and cyclic loading. These tests help

identify materials that can maintain structural stability, stiffness, and dimensional integrity under long-term service conditions. Extensive mechanical testing enables the selection of suitable materials for spiral wind turbine blades and helps create lightweight, high-strength, durable blade structures.

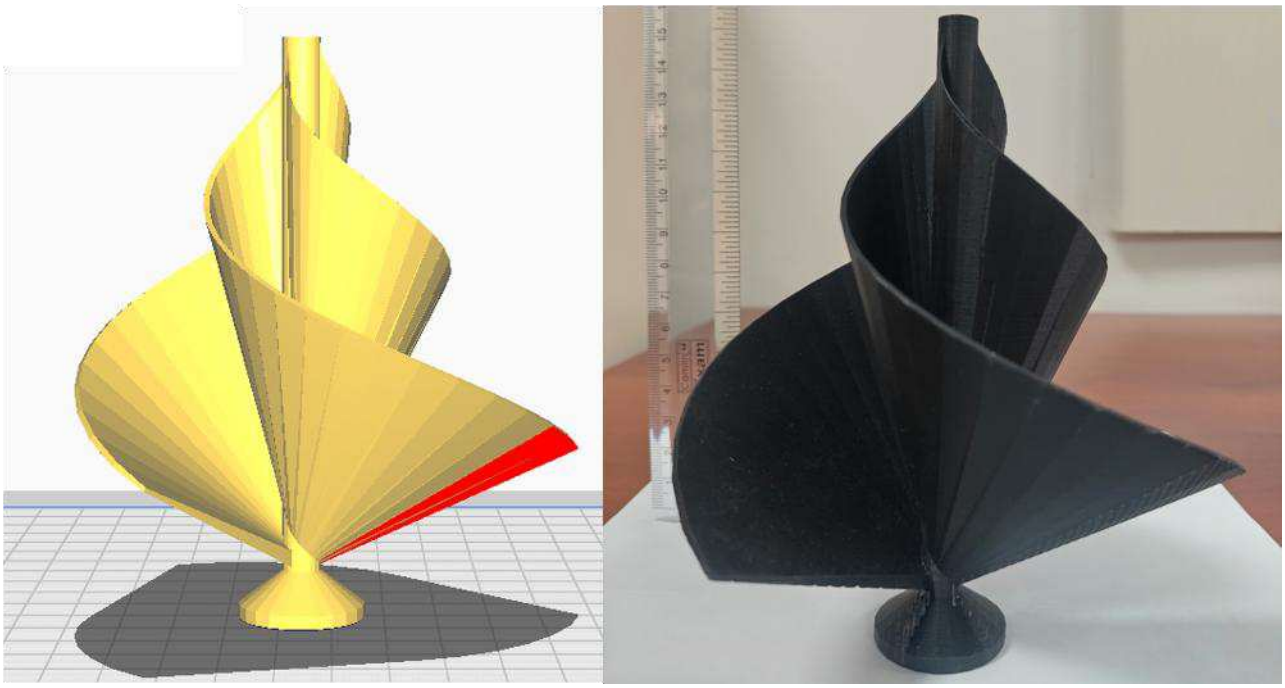


FIGURE 9 Prototype Spiral Wind Turbine Blade CAD and FFF-printed.

The selected CFPA material exhibits better mechanical behaviour, thermal stability, and structural resilience, and is therefore very suitable for renewable energy applications. The material provides a high strength-to-weight ratio compared with conventional fabricated structures, thereby improving blade efficiency and reducing overall structural weight.

Additionally, FFF allows direct fabrication of complex spiral blade geometry without the need for multiple assembly operations, FIGURE 9. The synergistic interaction between chopped CF reinforcement and a rectilinear deposition architecture enabled the development of structurally efficient thermoplastic composite systems with enhanced load-bearing capability and energy-absorption behaviour.

This significantly reduces manufacturing complexity, production time and material wastage while enhancing design flexibility and customisation. FFF is a promising approach for developing next-generation spiral wind turbine blades with improved aerodynamic and mechanical performance, as it enables the fabrication of lightweight, structurally efficient components with optimised internal lattice structures.

Conclusion

The present investigation demonstrated the potential of rectilinear infilled CFPA composites fabricated via FFF for lightweight wind turbine blade applications. The integration of chopped CF within the PA matrix significantly enhanced the thermal stability, structural integrity, and mechanical performance of the developed composites. The experimental results confirmed that the selected printing parameters and rectilinear infill structure contributed to improved interlayer bonding, dimensional consistency, and reliable material behaviour. Thermogravimetric analysis revealed excellent thermal stability and delayed degradation, indicating the suitability of CFPA composites for long-term operation under varying environmental conditions. X-ray diffractometry confirmed the presence of a stable semi-crystalline structure with effective reinforcement interaction and strong molecular bonding. Mechanical characterisation demonstrated that the FFF-printed CFPA specimens exhibited appreciable tensile, compressive, flexural, impact, and hardness properties, highlighting their ability to withstand different loading conditions encountered in wind turbine blade structures. The tensile and flexural studies indicated stable load-bearing capability and adequate stiffness, while the compression and impact analyses confirmed good energy absorption and progressive failure behaviour. Surface roughness evaluation further demonstrated uniform material deposition and a consistent surface morphology, both of which are essential for maintaining aerodynamic efficiency and reducing stress concentration during service conditions. This study establishes that rectilinear infilled CFPA composites possess a balanced combination of lightweight characteristics, mechanical strength, thermal stability, and surface quality, making them promising candidates for advanced wind turbine blade fabrication. The findings also highlight the capabilities of material extrusion-based AM to produce structurally efficient and sustainable composite components with reduced material waste and enhanced design flexibility. Future work may focus on fatigue behaviour, environmental ageing, and large-scale blade optimisation to further improve the applicability of CFPA composites in renewable energy systems.

Acknowledgement

The authors gratefully acknowledge the financial support provided by the **Ministry of Electronics and Information Technology (MeitY), Government of India**, under the **Centre for Promotion of Additive Manufacturing – Renewable Energy & Distributed Manufacturing (CPAM: RE & DM)** at the **Indian Institute of Technology (IIT) Mandi, MANDI (Himachal Pradesh), India**. The authors also acknowledge the facilities and technical support provided by the School of Computing and Electrical Engineering (SCEE), IIT Mandi, which enabled the successful completion of this research.

The authors gratefully acknowledge the support of the Design Laboratory for mechanical characterization, IIT Mandi Catalyst for FFF specimen fabrication, AMRC for XRD and TGA analyses, and C4DFED for surface roughness and FESEM characterization.

References

[1] U. Javaid, Z.M. Khan, M.B. Khan, M. Bassyouni, S.M.S. Abdel-Hamid, M.H. Abdel-Aziz, S.W. Ul Hasan, Fabrication and thermo-mechanical characterization of glass fiber/vinyl ester wind turbine rotor blade, Compos. Part B Eng. 91 (2016) 257–266. https://doi.org/10.1016/j.compositesb.2015.12.034.

[2] S. Rehman, L.M. Al-Hadhrami, M.M. Alam, J.P. Meyer, Empirical correlation between hub height and local wind shear exponent for different sizes of wind turbines, Sustain. Energy Technol. Assessments. 4 (2013) 45–51. https://doi.org/10.1016/j.seta.2013.09.003.

[3] H.K. Jang, W.H. Choi, C.G. Kim, J.B. Kim, D.W. Lim, Manufacture and characterization of stealth wind turbine blade with periodic pattern surface for reducing radar interference, Compos. Part B Eng. 56 (2014) 178–183. https://doi.org/10.1016/j.compositesb.2013.08.043.

[4] W.Q. Liu, X. liang Zhang, L. Gan, Cost-competitive incentives for wind energy development in China: institutional dynamics and policy changes, Int. J. Energy Technol. Policy. 1 (2002) 145–165. https://doi.org/10.1504/ijetp.2002.000807.

[5] D.U. Shah, P.J. Schubel, M.J. Clifford, Can flax replace E-glass in structural composites? A small wind turbine blade case study, Compos. Part B Eng. 52 (2013) 172–181. https://doi.org/10.1016/j.compositesb.2013.04.027.

[6] B.F. Towler, Wind Energy, in: Futur. Energy, Elsevier, 2014: pp. 187–214. https://doi.org/10.1016/B978-0-12-801027-3.00009-9.

[7] A. Jain, A. Sahai, R.S. Sharma, Enhancing the Mechanical Behaviour of Fused Filament Fabricated Carbon Fibre-Reinforced Poly-lactic Acid, J. Inst. Eng. Ser. D. 106 (2023) 115–122. https://doi.org/https://doi.org/10.1007/s40033-023-00498-3.

[8] A. Jain, T. Raj, A. Sahai, R.S. Sharma, Advancements in additive manufacturing for electrochemical energy storage devices, Proc. Inst. Mech. Eng. Part N J. Nanomater. Nanoeng. Nanosyst. (2025). https://doi.org/10.1177/23977914251361025.

[9] M.A. Saleh, R. Kempers, G.W. Melenka, A comparative study on the electromechanical properties of 3D-Printed rigid and flexible continuous wire polymer composites for structural health monitoring, Sensors Actuators A Phys. 328 (2021) 112764.

https://doi.org/10.1016/j.sna.2021.112764.

[10] H.K. Dave, B.H. Patel, S.R. Rajpurohit, A.R. Prajapati, D. Nedelcu, Effect of multi-infill patterns on tensile behavior of FDM printed parts, J. Brazilian Soc. Mech. Sci. Eng. 43 (2021) 1–15. https://doi.org/10.1007/s40430-020-02742-3.

[11] R.R. Fernandes, A.Y. Tamijani, M. Al-Haik, Mechanical characterization of additively manufactured fiber-reinforced composites, Aerosp. Sci. Technol. 113 (2021) 106653. https://doi.org/10.1016/j.ast.2021.106653.

[12] A. Jain, K. Pathik, S. Upadhyay, T. Raj, A. Sahai, R.S. Sharma, Machine Learning Approach in Fused Filament Fabrication for Flexural Characteristics of Polylactic Acid Reinforced with Carbon Fibres, Prog. Addit. Manuf. (2025). https://doi.org/10.1007/s40964-025-01078-5.

[13] A. Jain, A. Sahai, R.S. Sharma, Fracture morphology and strength characteristics of poly-lactic acid and poly-ethylene terephthalate glycol composites combined with taguchi method and response surface methodology, J. Thermoplast. Compos. Mater. 37 (2023) 2913–2943. https://doi.org/10.1177/08927057231221749.

[14] A. Jain, K. Kant, S.K. Singh, A. Sahai, R.S. Sharma, Process parameter tailored evaluation of FFF-fabricated carbon fibre based poly-lactic-acid composites, J. Thermoplast. Compos. Mater. 36 (2023) 4365–4387. https://doi.org/10.1177/08927057231155858.

[15] N. Mathiazhagan, N.K. Sivakumar, S. Palaniyappan, M. Rahaman, Influence of printing-based factors on the mechanical properties of hexagonal lattice-structured 3D printed novel walnut shell/polylactic acid composite, J. Thermoplast. Compos. Mater. 37 (2024) 713–742. https://doi.org/10.1177/08927057231185711.

[16] A. Jain, S. Upadhyay, A. Sahai, R.S. Sharma, Comparing the flexural and morphological properties of dissimilar FFF-fabricated polymer composites, J. Thermoplast. Compos. Mater. 37 (2023) 167–191. https://doi.org/10.1177/08927057231170790.

[17] A. Jain, T. Raj, A. Sahai, R.S. Sharma, Electrochemical energy storage device through fused filament fabrication: mechanical, electrical, and thermal characterisation, J. Mater. Sci. Mater. Electron. 37 (2026) 613. https://doi.org/10.1007/s10854-026-16960-3.

[18] S. Palaniyappan, D. Veeman, K. Rajkumar, K. Vishal, R. Kishore, L. Natrayan, Photovoltaic Industrial Waste as Substitutional Reinforcement in the Preparation of Additively Manufactured Acrylonitrile Butadiene Styrene Composite, Arab. J. Sci. Eng. 47 (2022) 15851–15863. https://doi.org/10.1007/s13369-022-06806-5.

[19] A. Jain, T. Raj, A. Sahai, R.S. Sharma, Structural behaviour of polyethylene

terephthalate glycol reinforced with carbon fibre through fused filament fabrication for automotive components, Plast. Rubber Compos. Macromol. Eng. (2025). https://doi.org/10.1177/14658011251353295.

[20] A. Jain, S. Upadhyay, A. Sahai, R.S. Sharma, Reinforcement-material effects on the compression behavior of polymer composites, J. Appl. Polym. Sci. 140 (2023) e53722. https://doi.org/10.1002/app.53722.

[21] D. Rajak, D. Pagar, P. Menezes, E. Linul, Fiber-Reinforced Polymer Composites: Manufacturing, Properties, and Applications, Polymers (Basel). 11 (2019) 1667. https://doi.org/10.3390/polym11101667.

[22] D.E. Samoylenko, K.S. Rodygin, V.P. Ananikov, Sustainable application of calcium carbide residue as a filler for 3D printing materials, Sci. Rep. 13 (2023) 4465. https://doi.org/10.1038/s41598-023-31075-z.

[23] A. Jain, A. Goyal, A. Raj, A. Rajora, L. Bhardwaj, A.S. Chandrakar, H. Gupta, P.K. Layal, T. Raj, G.S. Sharma, A. Sahai, R.S. Sharma, A Bibliometric Study of Additively Manufactured Batteries, Int. J. Interact. Des. Manuf. (2024). https://doi.org/https://doi.org/10.1007/s12008-024-02065-w.

[24] T. Raj, A. Jain, A. Sahai, R.S. Sharma, Influence of Printing Parameters on the Mechanical Properties of FFF-Printed PLA and PETG Composites, in: P.K. Kalra (Ed.), Parit. J. Syst. Sci. Eng., Systems Society of India, 2025.

[25] M.N. Islam, K.P. Baxevanakis, V. V. Silberschmidt, Mechanical characterisation of AM nylon-matrix carbon-fibre-reinforced composite in tension, Mater. Today Proc. 70 (2022) 50–54. https://doi.org/10.1016/j.matpr.2022.08.527.

[26] I. Buj-Corral, E.E. Zayas-Figueras, Comparative study about dimensional accuracy and form errors of FFF printed spur gears using PLA and Nylon, Polym. Test. 117 (2023) 107862. https://doi.org/10.1016/j.polymertesting.2022.107862.

[27] A. Yankin, G. Serik, S. Danenova, Y. Alipov, A. Temirgali, D. Talamona, A. Perveen, Optimization of Fatigue Performance of FDM ABS and Nylon Printed Parts, Micromachines. 14 (2023) 304. https://doi.org/10.3390/mi14020304.

[28] S. Guessasma, S. Belhabib, H. Nouri, Effect of printing temperature on microstructure, thermal behavior and tensile properties of 3D printed nylon using fused deposition modeling, J. Appl. Polym. Sci. 138 (2021). https://doi.org/10.1002/app.50162.

[29] F. Ning, W. Cong, Z. Jia, F. Wang, M. Zhang, Additive manufacturing of CFRP composites using fused deposition modeling: Effects of process parameters, ASME 2016 11th Int. Manuf. Sci. Eng. Conf. MSEC 2016. 3 (2016) 1–7.

https://doi.org/10.1115/MSEC20168561.

[30] N.M. Cococcetta, D. Pearl, M.P. Jahan, J. Ma, Investigating surface finish, burr formation, and tool wear during machining of 3D printed carbon fiber reinforced polymer composite, J. Manuf. Process. 56 (2020) 1304–1316. https://doi.org/10.1016/j.jmapro.2020.04.025.

[31] K. Yadav, V. Tiwari, Effects of voids on mechanical response and failure behaviour of additively manufactured Onyx, Prog. Addit. Manuf. 10 (2025) 8591–8620. https://doi.org/10.1007/s40964-025-01139-9.

[32] S.R. Piramanayagam, M. Kalimuthu, R. Nagarajan, A.M. Abdul Karim Sait, R.K. Krishnamoorthy, S.O. Ismail, S. Siengchin, F. Mohammad, H.A. Al-Lohedan, Experimental investigation and statistical analysis of additively manufactured onyx-carbon fiber reinforced composites, J. Appl. Polym. Sci. 138 (2021). https://doi.org/10.1002/app.50338.

[33] D. Nikiema, P. Balland, A. Sergent, Study of the Mechanical Properties of 3D-printed Onyx Parts: Investigation on Printing Parameters and Effect of Humidity, Chinese J. Mech. Eng. Addit. Manuf. Front. 2 (2023) 100075. https://doi.org/10.1016/j.cjmeam.2023.100075.

[34] Y. Peng, Y. Wu, S. Li, K. Wang, S. Yao, Z. Liu, H. Garmestani, Tailorable rigidity and energy-absorption capability of 3D printed continuous carbon fiber reinforced polyamide composites, Compos. Sci. Technol. 199 (2020) 108337. https://doi.org/10.1016/j.compscitech.2020.108337.

[35] G. Liu, Y. Xiong, L. Zhou, Additive manufacturing of continuous fiber reinforced polymer composites: Design opportunities and novel applications, Compos. Commun. 27 (2021) 100907. https://doi.org/10.1016/j.coco.2021.100907.

[36] Y. Liu, W. Jiang, W. Hu, L. Ren, E. Deng, Y. Wang, C. Song, Q. Feng, Compressive strength and energy absorption characteristics of the negative stiffness honeycomb cell structure, Mater. Today Commun. 35 (2023) 105498. https://doi.org/10.1016/j.mtcomm.2023.105498.

[37] K.I. Ismail, T.C. Yap, R. Ahmed, 3D-Printed Fiber-Reinforced Polymer Composites by Fused Deposition Modelling (FDM): Fiber Length and Fiber Implementation Techniques, Polymers (Basel). 14 (2022) 4659. https://doi.org/10.3390/polym14214659.

[38] A. Das, M. Etemadi, B.A. Davis, S.H. McKnight, C.B. Williams, S.W. Case, M.J. Bortner, Rheological investigation of nylon-carbon fiber composites fabricated using

material extrusion-based additive manufacturing, Polym. Compos. 42 (2021) 6010–6024. https://doi.org/10.1002/pc.26281.

[39] A. Anbalagan, E.J. Launchbury, M. Kauffman, A. Pazhani, M. Anthony Xavior, Investigation on CFRP 3D printing build parameters and their effect on topologically optimised complex models, Mater. Today Proc. (2023). https://doi.org/10.1016/j.matpr.2023.04.352.

[40] S. Sangaletti, M.T. Aranda, L. Távara, I.G. García, Effect of stacking direction and raster angle on the fracture properties of Onyx 3D printed components: A mesoscale analysis, Theor. Appl. Fract. Mech. 129 (2024) 104228. https://doi.org/10.1016/j.tafmec.2023.104228.

[41] Y. Tao, F. Kong, Z. Li, J. Zhang, X. Zhao, Q. Yin, D. Xing, P. Li, A review on voids of 3D printed parts by fused filament fabrication, J. Mater. Res. Technol. 15 (2021) 4860–4879. https://doi.org/10.1016/j.jmrt.2021.10.108.

[42] H. Gonabadi, S.F. Hosseini, Y. Chen, S. Bull, Size effects of voids on the mechanical properties of 3D printed parts, Int. J. Adv. Manuf. Technol. 132 (2024) 5439–5456. https://doi.org/10.1007/s00170-024-13683-9.

[43] J.M. Pappas, A.R. Thakur, M.C. Leu, X. Dong, A parametric study and characterization of additively manufactured continuous carbon fiber reinforced composites for high-speed 3D printing, Int. J. Adv. Manuf. Technol. 113 (2021) 2137–2151. https://doi.org/10.1007/s00170-021-06723-1.

[44] D.R. Hetrick, S.H.R. Sanei, C.E. Bakis, O. Ashour, Evaluating the effect of variable fiber content on mechanical properties of additively manufactured continuous carbon fiber composites, J. Reinf. Plast. Compos. 40 (2021) 365–377. https://doi.org/10.1177/0731684420963217.

[45] J.M. Barrios, P.E. Romero, Improvement of surface roughness and hydrophobicity in PETG parts manufactured via fused deposition modeling (FDM): An application in 3D printed self-cleaning parts, Materials (Basel). 12 (2019). https://doi.org/10.3390/ma12152499.

[46] J. Ji, C. Zhang, X. Zhang, Y. Chen, Recent research advances in wind turbine thermal management technologies, Renew. Sustain. Energy Rev. 208 (2025) 114983. https://doi.org/10.1016/j.rser.2024.114983.

[47] E. Zavvar, P. Rosa-Santos, F. Taveira-Pinto, E. Ghafoori, Lifetime extension of offshore support structures of wind turbines: A review, Renew. Sustain. Energy Rev. 217 (2025) 115788. https://doi.org/10.1016/j.rser.2025.115788.

[48] T.A. Badea, L.R. Maier, A.-A. Crisan, Assessment of Additively Manufactured Thermoplastic Composites for Ablative Thermal Protection Systems (TPSs), Polymers (Basel). 17 (2025) 2338. https://doi.org/10.3390/polym17172338.

[49] B. Ben Fraj, Z. Ahmed, Thermal, Structural, and Mechanical Properties of Carbon Fiber Reinforced PLA Composites: Influence of FDM Print Speed and Comprehensive Analysis, Polym. Compos. 46 (2025) 17229–17239. https://doi.org/10.1002/pc.70107.

[50] Z. Rbihi, F. Erchiqui, D. Rodrigue, H. Kaddami, Thermal, Mechanical, and Rheological Properties of PLA/PHB Biocomposites Reinforced with Alkaline-Treated Hemp Fibers and Granules, ChemEngineering. 9 (2025) 122. https://doi.org/10.3390/chemengineering9060122.

[51] L. Yin, J. Chen, J. Xie, R. Xu, C. Lei, Tensile Yielding and Hardening in Semi-Crystalline Polymers: Synergistic Effects of Amorphous Entangled Network and Tie-Chain Network, Macromolecules. 59 (2026) 4374–4386. https://doi.org/10.1021/acs.macromol.6c00389.

[52] L.L. Dawood, E.S. AlAmeen, Influence of infill patterns and densities on the fatigue performance and fracture behavior of 3D-printed carbon fiber-reinforced PLA composites, AIMS Mater. Sci. 11 (2024) 833–857. https://doi.org/10.3934/matersci.2024041.

[53] S. Dabees, L.C. Henderson, D.J. Hayne, Carbon fibre surface modification and its effects on adhesion, mechanical, and tribological behaviour of high-performance thermoplastics, Compos. Part B Eng. 306 (2025) 112758. https://doi.org/10.1016/j.compositesb.2025.112758.

[54] L. Chanraksmey, W. Zhao, Y. Han, Y. Chen, O. Ghita, B. Chen, Recent advances in additive manufacturing of impact-resistant structures with high-performance polymers and their composites, Addit. Manuf. Front. 5 (2026) 200276. https://doi.org/10.1016/j.amf.2025.200276.

[55] M. Kurokawa, Y. Uchiyama, T. Iwai, S. Nagai, Performance of plastic gear made of carbon fiber reinforced polyamide 12, Wear. 254 (2003) 468–473. https://doi.org/10.1016/S0043-1648(03)00020-6.

[56] Impact of Surface Roughness on the Aerodynamic Efficiency of Wind Turbines: A New CFD-based Correlation, J. Appl. Fluid Mech. 18 (2025). https://doi.org/10.47176/jafm.18.2.2830.

[57] X. Cheng, B. Du, J. He, W. Long, G. Su, J. Liu, Z. Fan, L. Chen, A review of thermoplastic composites on wind turbine blades, Compos. Part B Eng. 299 (2025)

112411. https://doi.org/10.1016/j.compositesb.2025.112411.

[58] J. Lambert, A.R. Chambers, I. Sinclair, S.M. Spearing, 3D damage characterisation and the role of voids in the fatigue of wind turbine blade materials, Compos. Sci. Technol. 72 (2012) 337–343. https://doi.org/10.1016/j.compscitech.2011.11.023.

[59] D. Yang, H. Zhang, J. Wu, E.D. McCarthy, Fibre flow and void formation in 3D printing of short-fibre reinforced thermoplastic composites: An experimental benchmark exercise, Addit. Manuf. 37 (2021) 101686. https://doi.org/10.1016/j.addma.2020.101686.